Gait & Posture 73 (2019) 221–227

Contents lists available at ScienceDirect

Gait & Posture

journal homepage: www.elsevier.com/locate/gaitpost

Full length article

A robust machine learning enabled decomposition of shear ground reaction forces during the double contact phase of walking

Guillaume J. Bastien[a,b], Thierry P. Gosseye[a,b], Massimo Penta[a,b,*]

[a] Institute of Neuroscience, Université catholique de Louvain, Louvain-la-Neuve, Belgium
[b] Arsalis SPRL, Glabais, Belgium

ARTICLE INFO

Keywords:
Walking
Double contact
Ground reaction force
Decomposition
Machine learning

ABSTRACT

Background: Dynamic analyses of walking rely on the 3D ground reaction forces (GRF) under each foot, while only the resultant force of both limbs may be recorded on a single-belt instrumented treadmill or when both feet touch the same force platform.
Research question: This study aims to develop a robust decomposition of the shear GRF to complete the most accurate decomposition of the vertical GRF [8].
Methods: A retrospective study of 374 healthy adults records (age: 22.8 ± 2.6 years, speed: 1.34 ± 0.28 m/s) and of 434 patient records (age: 21.3 ± 17.8 years, speed: 0.64 ± 0.19 m/s) were used in a machine learning process to develop a robust predictive model to decompose the fore-aft GRF. The lateral GRF was decomposed by resolving the equilibrium of transverse moments around the center of pressure.
Results: A predictive linear model of the fore-aft GRF under the back foot every 5% of the double contact phase was obtained from 2 predictors: the total fore-aft GRF and the vertical GRF under the back foot. Each predictor uses a time series of 31 samples before and during the double contact. The model performs accurately in healthy (median[IQR] error of 3.0[2.2–4.1]%) and in clinical gaits (7.7[4.7–13.4]%). The error in lateral GRF decomposition is of 5.7[3.9–10.2]% in healthy gaits and of 12.0[7.2–19.2]% in patients under the back foot and about half of that under the front foot.
Significance: The decomposition of shear GRFs achieved in this study supports the mechanics of walking. It provides outstanding accuracy in healthy gait and also applies to neurologic and orthopedic disorders. Together with the vertical GRF decomposition [8], this approach for the shear components paves the way for robust single limb GRF determination on a single-belt instrumented treadmill or when both feet touch the same force platform in normal and clinical gait analysis.

1. Introduction

Human walking is characterized by alternating phases of single and double foot contact on the floor. The ground reaction forces are recorded while walking on force platforms or on an instrumented treadmill in order to characterize the gait, to detect asymmetries and to assess clinical gaits. Nevertheless, some gait parameters such as the peak force under one foot or the joint torques derived using inverse dynamics, require the knowledge of the ground reaction force under each foot; which cannot be measured directly when both feet are in contact with a single force sensor. Several approaches have been proposed to overcome this limitation. First, force platforms are laid in a pattern that allows the subject to step with each foot on independent platforms. Second, split-belt instrumented treadmills have been developed to record the ground reaction force under each foot while walking across a separation line between independent force platforms built into the treadmill. Both approaches may lead to “targeting” behaviors where the subjects tend to aim for a fixed platform or to avoid the separation line, resulting in a significant alteration in the ground reaction force measurement [1,2].

A third approach consists in recording the ground reaction force during the double contact phase with a single sensor and computationally decomposing the recorded signal into signals for each individual foot. This approach is especially useful for recording numerous steps of gait on a single-belt instrumented treadmill while avoiding the problem of "targeting" the foot strikes [3–5]. Algorithms used to achieve this decomposition are typically built from individual foot force records summed as if they were obtained with a single sensor during the double

* Corresponding author at: Institute of Neuroscience, Université catholique de Louvain, Louvain-la-Neuve, Belgium, Place de Coubertin, 1 bte L8.10.01, B-1348 Louvain-la-Neuve, Belgium.
E-mail address: massimo.penta@uclouvain.be (M. Penta).

https://doi.org/10.1016/j.gaitpost.2019.07.190
Received 20 December 2018; Received in revised form 19 June 2019; Accepted 8 July 2019

contact phase of walking. Then, the total force is decomposed computationally and validated against the measured signals. Some decomposition algorithms only address the vertical component of the ground reaction force [6–8]. To date, the smallest error in the decomposition of the vertical component of the ground reaction force has a median relative error of 1.8% in healthy gait and of 2.5% in clinical gait, strictly determined by the error on the center of pressure under each foot [8].

Decomposition algorithms for the shear components of the ground reaction forces, namely the foreaft and the lateral components, have been proposed more recently [9–11]. All algorithms use curve fitting techniques to best match the force components recorded under each individual foot. Existing algorithms [9,10] fit the ground reaction force recorded under the back foot, since it is typically smoother than that under the front foot and one of them [11] uses additional characteristic points of the recorded signals to resolve the undetermined parameters of the fitted curve. To date, the smallest average root mean square error reached is over 6% in the fore-aft direction and between 7% and 18% in the lateral direction. Samadi et al. [10] report relative errors of the same magnitudes, but computed relative to the amplitude of the total force recorded under both feet rather than relative to the single foot force; which complicates the performance comparison. A shortcoming of most of these algorithms is that they disregard the necessary equilibrium of the moments around a vertical axis. Indeed, the only study that assessed the error in moments [9] reports the largest errors in the lateral force (18%) and in the transverse moment (over 12%), most likely due the interdependence of these kinetic components.

Another limitation of most algorithms [9,10] is that they merely provide the best fit on their data, i.e. best performance model, but they fail to address the robustness of the model in new data of the same kind. Machine learning techniques include predictive models that can be used to define a function relating a predicted variable to a set of predictors [12]. In walking, the ground reaction force component under one foot could be predicted from a set of predictors such as the total ground reaction force under both feet, size or speed. Besides determining the performance of a given model, i.e. its error, these techniques can also be used to address the model robustness. Typically, a part of the dataset is used to fit the highest performance model, and another part is used to validate the model performance on 'new' data in order to confirm the model performance in the validation sample [13,14]; the more robust models are obtained when the performance is equal in the training sample and in the validation sample [15].

The objective of this paper is to develop a robust predictive decomposition of the shear components of the ground reaction force under each foot during the double contact phase of walking.

2. Material and methods

2.1. Subjects and procedures

A retrospective study was carried out on a total of 808 force platform records from 27 healthy adults and 88 patients including 33 adults and 55 children (see Table 1). The healthy subjects had no injury of the locomotor system and no history of neurological disorder at the time of assessment. The study was conducted according to the Declaration of Helsinki and was approved by the local ethics committee. For the recordings, the subjects walked on a force platform at a speed ranging from 0.83 to 1.94 m/s; the patients walked at their spontaneous speed. The records with both feet on separate force plates were used for this study. The three-dimensional ground reaction force (GRF) and center of pressure (COP) under each foot were recorded at 250 Hz or 500 Hz for the healthy subjects and at 50 Hz for the patients, from different force platforms [16–18], after the analog force signals had been filtered with an 8-pole Bessel low pass filter with a cutoff frequency of 125 Hz. All signals were resampled at 1 kHz for the analysis. The timing of the double contact (DC) phase was determined from the front foot contact (FC, i.e. when the vertical GRF under the front foot exceeds 10 N) until the back foot off (FO, i.e. when the vertical GRF under the back foot falls below 10 N) and was then normalized (0% = FC, 100% = FO). The GRF recorded under both feet were normalized in body weight units and summed to obtain the total GRF. Then, the vertical component of the GRF was decomposed to compute the force under each foot, $\hat{F}_{z,back}$ and $\hat{F}_{z,front}$, assuming that the COP under each foot remained fix during the DC: the COP of the back foot was fixed at its position at the FC; the COP of the front foot was fixed at its position at the FO [8]. Notations with a "^" accent indicate decomposed values, notations without accent indicate actually measured signals.

Table 1
Sample characteristics.

	Healthy	Patients
Sample size, n subjects / n steps		
Adults	27 / 374	33 / 168
Children	–	54 / 266
Age, year (mean ± sd)		
Adults	22.8 ± 2.6	39.8 ± 16.0
Children	–	9.5 ± 3.0
Body weight, kg (mean ± sd)		
Adults	71.6 ± 9.5	67.3 ± 16.7
Children	–	30.3 ± 12.7
Walking speed, m/s (mean ± sd)		
Adults	1.34 ± 0.28	0.57 ± 0.19
Children	–	0.67 ± 0.19
Neurological pathologies, n patients / n steps		
Periventricular leukomalacia	–	2 / 10
Idiopathic toe-walker	–	2 / 11
Hemiplegia	–	24 / 117
Diplegia	–	7 / 42
Cerebral palsy	–	28 / 123
Arnold-Chiari malformation	–	1 / 5
Myopathy	–	1 / 7
Paraparesis	–	3 / 17
Childhood polio	–	1 / 5
Quadriparesis	–	2 / 12
Orthopedic pathologies, n patients / n steps		
Ankle sprain	–	2 / 10
Osteoarthritis of the knee	–	1 / 4
Lower limb fracture	–	1 / 7
Spondylolysis	–	1 / 7
Equinovarus	–	4 / 16
Foot valgus	–	1 / 11
Spasticity	–	1 / 8
Other pathologies, n patients / n steps		
Fibromyalgia	–	2 / 10
Walking unstable	–	2 / 9
Psychomotor retardation	–	1 / 3

2.2. Decomposition of the fore-aft ground reaction force component

A machine learning model was applied to predict the fore-aft GRF on the back foot ($F_{y,back}$) by computing a set of 19 predicted $\hat{F}_{y,back}$ values at 5% intervals during the DC. The model has been evaluated according to a leave-one-subject-out cross validation by determining the model parameters on training data (all but one subject left-out) within each fold of the cross validation and by assessing the model performance on test data (the left-out subject) (14). Five sets of variables were initially considered as predictors: the total GRF in lateral ($F_{x,tot}$) and fore-aft ($F_{y,tot}$) directions, the decomposed vertical GRF under each foot ($\hat{F}_{z,back}$ and $\hat{F}_{z,front}$) and the total frictional torque around the COP ($T_{z,tot}$). Each predictor was a time series of 31 samples including 10 samples at 4 ms intervals during the 40 milliseconds prior to the DC and 21 samples at 5% intervals between 0 and 100% of the DC. Using a nested leave-one-subject-out cross validation [13,14], a backward stepwise selection on training data showed that only $F_{y,tot}$ and $\hat{F}_{z,back}$ were sufficient to minimize the validation error (within 3% of the minimum error), leading to a total of 2*31 predictor values.

The model used to predict the fore-aft GRF under the back foot at 19 instants t (t ∈ {5%–95% of the DC in increments of 5%}) during the DC for a given step s is presented below:

$$\begin{bmatrix} \hat{F}_{y,back,5\%,s} \\ \vdots \\ \hat{F}_{y,back,95\%,s} \end{bmatrix} = \begin{bmatrix} C_{1,1,5\%} & \cdots & C_{1,31,5\%} & C_{2,1,5\%} & \cdots & C_{2,31,5\%} \\ \vdots & \ddots & \vdots & \vdots & \ddots & \vdots \\ C_{1,1,95\%} & \cdots & C_{1,31,95\%} & C_{2,1,95\%} & \cdots & C_{2,31,95\%} \end{bmatrix} \cdot \begin{bmatrix} F_{y,tot,1,s} \\ \vdots \\ F_{y,tot,31,s} \\ \hat{F}_{z,back,1,s} \\ \vdots \\ \hat{F}_{z,back,31,s} \end{bmatrix}$$

where $\hat{F}_{y,back,t,s}$ is the decomposed fore-aft GRF under the back foot at instant t of the DC for step s; $F_{y,tot,n,s}$ and $\hat{F}_{z,back,n,s}$ are the values of the predictors at the nth sample (n ∈ {1–31}) for step s and $C_{v,n,t}$ is the coefficient of the nth sample of predictor v (1 for $F_{y,tot}$ and 2 for $\hat{F}_{z,back}$) to predict $\hat{F}_{y,back}$ at instant t of the DC.

The coefficients $C_{v,n,t}$ have been determined by solving the learning model that regresses the $F_{y,back,t,s}$ actually recorded under the back foot at instant t of the DC of step s against the 62 predictor values (31 for $F_{y,tot}$ and 31 for $\hat{F}_{z,back}$) for the k steps of the training dataset, as follows:

$$\begin{bmatrix} F_{y,back,t,1} \\ \vdots \\ F_{y,back,t,k} \\ 0 \\ 0 \\ \vdots \\ 0 \\ 0 \end{bmatrix} = \begin{bmatrix} F_{y,tot,1,1} & F_{y,tot,2,1} & \cdots & F_{y,tot,31,1} & \hat{F}_{z,back,1,1} & \cdots & \hat{F}_{z,back,30,1} & \hat{F}_{z,back,31,1} \\ \vdots & \vdots & \ddots & \vdots & \vdots & \ddots & \vdots & \vdots \\ F_{y,tot,1,k} & F_{y,tot,2,k} & \cdots & F_{y,tot,31,k} & \hat{F}_{z,back,1,k} & \cdots & \hat{F}_{z,back,30,k} & \hat{F}_{z,back,31,k} \\ \lambda & 0 & \cdots & 0 & 0 & \cdots & 0 & 0 \\ 0 & \lambda & \cdots & 0 & 0 & \cdots & 0 & 0 \\ \vdots & \vdots & \ddots & \vdots & \vdots & \ddots & \vdots & \vdots \\ 0 & 0 & \cdots & 0 & 0 & \cdots & \lambda & 0 \\ 0 & 0 & \cdots & 0 & 0 & \cdots & 0 & \lambda \end{bmatrix} \cdot \begin{bmatrix} C_{1,1,t} \\ C_{1,2,t} \\ \vdots \\ C_{1,31,t} \\ C_{2,1,t} \\ \vdots \\ C_{2,30,t} \\ C_{2,31,t} \end{bmatrix}$$

When using only the first k lines of the matrix equation, the coefficients $C_{v,n,t}$ associated with each predictor showed substantial jitter as a function of time, indicating that the non-orthogonal predictors tended to overfit the regression. A smoother predictive model for $\hat{F}_{y,back}$ was obtained by including a ridge regularization [19] in the learning model, as shown by the last 62 lines of the matrix equation. Each coefficient $C_{v,n,t}$ is weighted with the ridge parameter (λ) which tends to minimize the sum of the squares of all coefficients $C_{v,n,t}$ and reduce the coefficients variation throughout the DC. The same value for λ has been used in a comparable learning model for the 19 instants t during the DC.

A nested leave-one-subject-out cross validation [13,14] was performed repeatedly with the λ parameter increasing from zero until the training error (i.e. the average normalized error in the training data) was equal to the validation error (i.e. the average normalized error in the validation steps) denoting a statistical robustness [15]. The equivalence was tested with two one-sided tests (TOST) [20,21] using an equivalence interval of ± 10% of the mean learning error. The level of statistical significance was set to 0.05.

The values of $\hat{F}_{y,back}$ computed with the predictive model at 19 instants t were then interpolated with a cubic spline to determine the instantaneous value for $\hat{F}_{y,back}$ throughout the DC. This value was then subtracted from the total fore-aft GRF to determine the force under the front foot ($\hat{F}_{y,front}$).

2.3. Decomposition of the lateral ground reaction force component

The lateral component of the GRF was determined by resolving the equilibrium of transverse moments. During the DC, the total moment ($T_{z,tot}$) recorded by the force platform around a vertical axis collinear with the center of pressure can be expressed as:

$$T_{z,tot} = F_{y,back}.(OP_{x,back} - OP_{x,tot}) - F_{x,back}.(OP_{y,back} - OP_{y,tot}) + T_{z,back} + F_{y,front}.(OP_{x,front} - OP_{x,tot}) - F_{x,front}.(OP_{y,front} - OP_{y,tot}) + T_{z,front}$$

where $F_{d,f}$ is the GRF component and $OP_{d,f}$ is the coordinate of the COP, respectively, in direction d under foot f (i.e. 'front', 'back' or 'tot' for both feet) and $T_{z,f}$ is the frictional torque under foot f during the DC. The $T_{z,tot}$ consists of three components: the moment due to the offset between the COP under both feet (expressed by the shear GRF components) and the frictional torque under the front ($T_{z,front}$) and the back foot ($T_{z,back}$). During the DC, $T_{z,back}$ is initially equal to $T_{z,tot}$ and then decreases to zero, while $T_{z,front}$ is initially null and increases to be equal to $T_{z,tot}$ at the end of the DC. A linear interpolation was used for both $\hat{T}_{z,front}$ and $\hat{T}_{z,back}$ during the DC as the simplest realistic hypothesis. By considering the decomposed $\hat{F}_{y,back}$, the assumed $\hat{T}_{z,front}$ and $\hat{T}_{z,back}$ and the coordinates of the COP under each foot during the DC [8], this equation could be solved for $\hat{F}_{x,back}$ as follows:

$$\hat{F}_{x,back} = \frac{1}{\hat{OP}_{y,front} - \hat{OP}_{y,back}}.(T_{z,tot} - \hat{T}_{z,front} - \hat{T}_{z,back} - \hat{F}_{y,back}.(\hat{OP}_{x,back} - \hat{OP}_{x,front}) - F_{y,tot}.(\hat{OP}_{x,front} - OP_{x,tot}) + F_{x,tot}.(\hat{OP}_{y,front} - OP_{y,tot}))$$

The force under the front foot ($\hat{F}_{x,front}$) was computed by subtracting $\hat{F}_{x,back}$ from $F_{x,tot}$.

2.4. Decomposition error

The absolute error was computed for both decomposed shear components as the absolute difference between the decomposed and the recorded GRF under any foot. The normalized error was computed by dividing the absolute error by the subject body weight. While the absolute and normalized errors are identical for both feet, the relative error was determined by dividing the mean absolute error in each direction by the peak-to-peak force variation recorded under each foot in that direction during the DC.

3. Results

The result of the leave-one-subject-out cross validation used to determine $\hat{F}_{y,back}$ on the 808 steps is illustrated in Fig. 1. It shows a mean body weight normalized error on the whole dataset of 78 mN/kg without ridge regularization (λ = 0). The mean validation error on all single steps is systematically higher than the learning error. Higher values of λ tend to bring both errors closer to one another, hence producing a more robust model with smaller variations of the regression coefficients across the DC. A robust prediction demonstrating a significant equivalence of the validation and learning error (± 10%

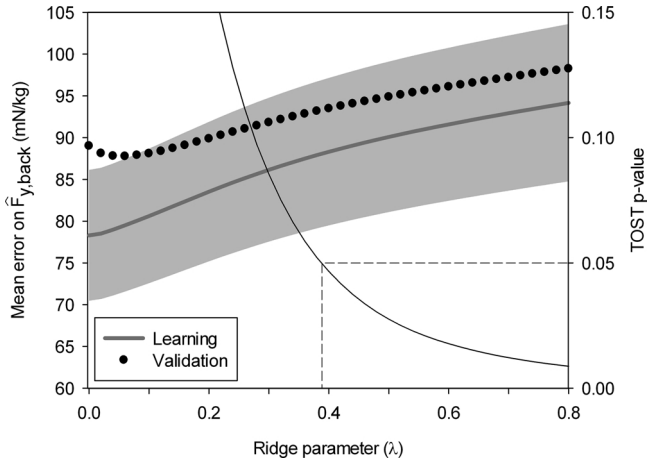

Fig. 1. The mean body weight normalized error on $\hat{F}_{y,back}$ of the learning model (thick grey curve) including a ± 10% equivalence interval (light grey area) is compared with the mean normalized error in all validation steps (black circles) including normal and clinical gaits. Without ridge regularization ($\lambda = 0$), both errors substantially differ indicating that the predictive model lacks robustness. Higher ridge regularizations demonstrate validation errors closer to the learning errors according to a decreasing p-value of the two one-sided tests (TOST, thin black curve, right-side ordinate). A robust learning model, with a significant equivalence of the mean relative validation and learning errors (TOST p-value < 0.05) was obtained with a λ of 0.388 (dashed line).

equivalence interval, TOST p-value < 0.05) was obtained for a ridge parameter of 0.388.

The values of coefficients $C_{v,n,t}$ of the predictive model for $\hat{F}_{y,back}$ computed with a λ of 0.388 are illustrated in Fig. 2. Among the time series of the $F_{y,tot}$ samples used to predict $\hat{F}_{y,back}$, the most important determinants are those with the higher absolute value (red and dark blue in Fig. 2), i.e. the samples around the beginning of the DC, the samples in phase with $\hat{F}_{y,back}$ between 40 and 80% of the DC and the samples that just precede the end of the DC. Among the time series of the $\hat{F}_{z,back}$ samples used to predict $\hat{F}_{y,back}$, the most important determinants are the samples at the very beginning of the DC and the samples between 25 and 75% of the DC that slightly anticipate or are in phase the predicted value of $\hat{F}_{y,back}$.

A typical trace illustrating the decomposition of the three GRF components is presented in Fig. 3. It shows that the computational decomposition is able to determine slow GRF changes as measured under the rear foot in the fore-aft direction as well as faster changes as measured in the fore-aft direction under the front foot and in the lateral direction.

The normalized error on the decomposition of the shear GRFs is presented in Fig. 4. The results indicate that the median error is the highest around the middle of the DC phase. Noticeably, the median error in the fore-aft direction is quite comparable in normal and in clinical gaits, although the error distribution is more spread in clinical gaits. In the lateral direction, the normalized error in clinical gait is twice as high as in healthy controls. The absolute and relative decomposition errors are also presented in Table 2. The median relative error on the decomposition of the foreaft GRF is lower than 3.0% under either foot in normal gait and lower than 7.7% in clinical gait. The relative error is less symmetrical for the lateral than for the fore-aft GRF: the median relative error is of 5.7% in normal gaits and of 12.0% in clinical gaits under the back foot, while it is about half of that under the front foot.

4. Discussion

A method has been proposed to decompose the ground reaction force (GRF) under each foot while recording only the total GRF under both feet on a force platform during the double contact (DC) phase of walking. After determining the timing of the single and double contact, the decomposition of the GRF components is approached sequentially: first the vertical GRF is decomposed [8], then a prediction model is used for the foreaft GRF and then the equilibrium of transverse moments around the center of pressure (COP) is used for the lateral GRF.

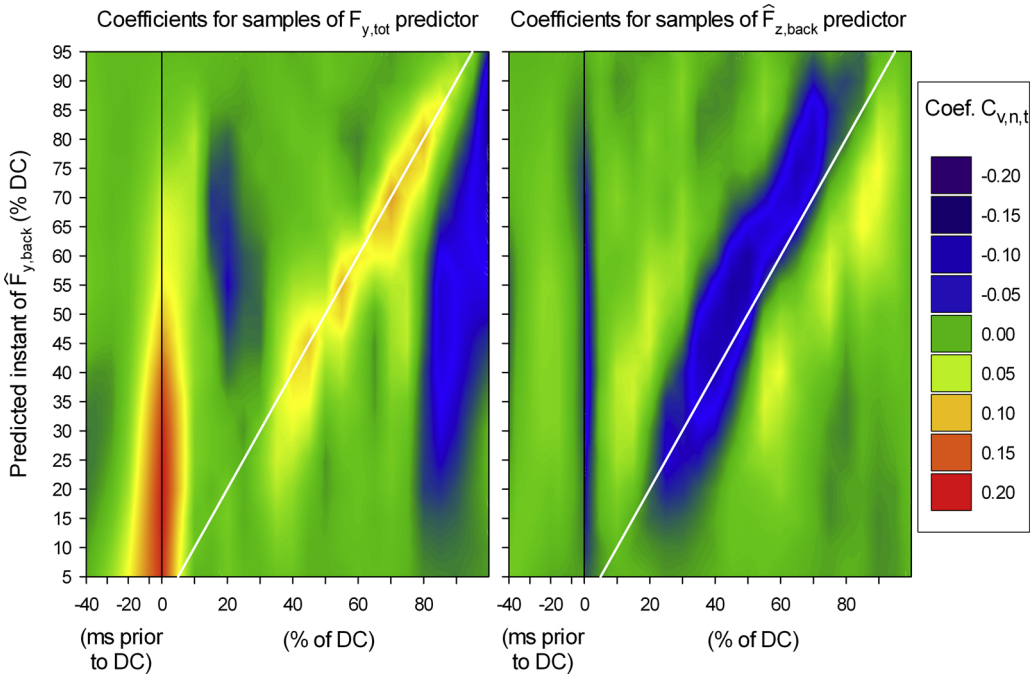

Fig. 2. Regression coefficients $C_{v,n,t}$ for both predictor variables, $F_{y,tot}$ (left panel) and $\hat{F}_{z,back}$ (right panel) used to determine $\hat{F}_{y,back}$ during the DC phase of walking. The model determines the value of $\hat{F}_{y,back}$ from 5% to 95% of the DC in 5% increments (ordinate) using a linear regression of 31 samples of each predictor variable (10 samples during the 40 ms prior to the DC and of 21 samples from 0% to 100% of the DC) (abscissas). The white line in each plot indicates instants where each predictor is synchronous with the predicted value of $\hat{F}_{y,back}$.

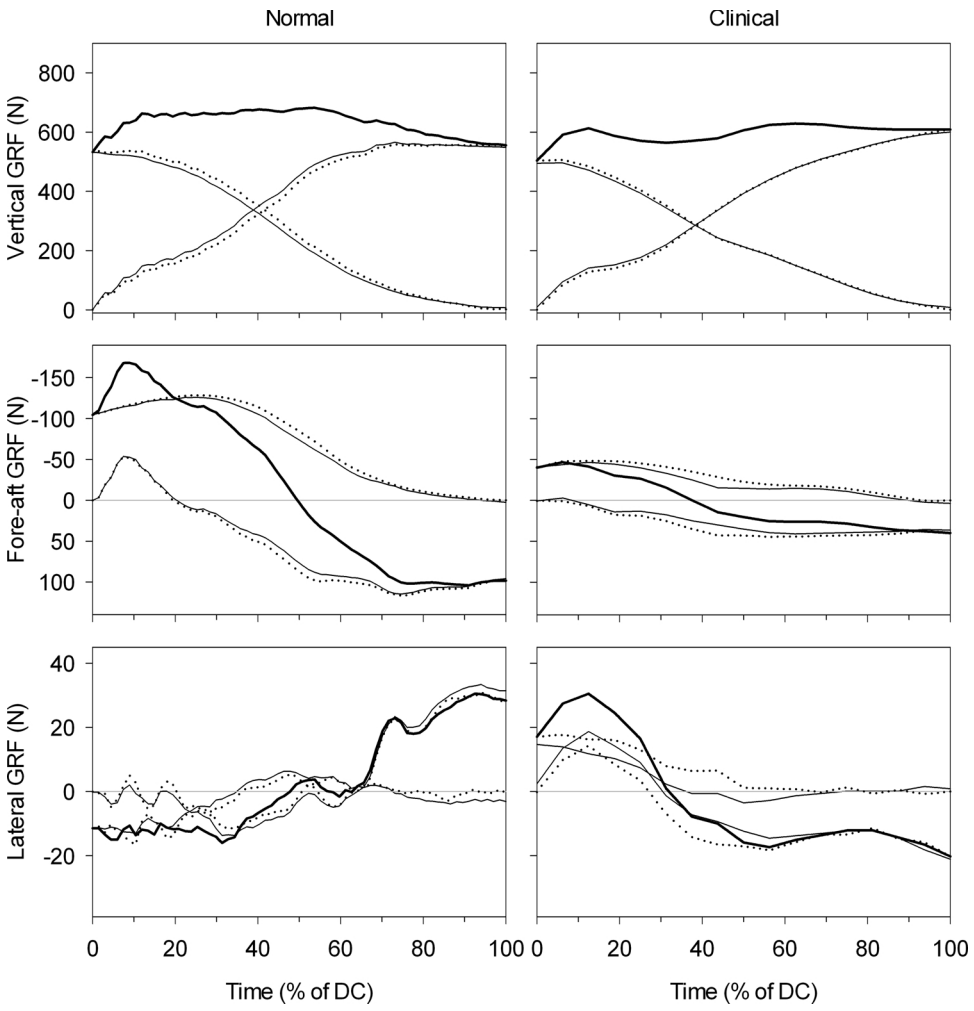

Fig. 3. Typical traces of the vertical, foreaft and lateral GRF during the DC in normal gait for a healthy subject walking at 1.33 m/s (left panels) and in clinical gait for a patient walking at 0.28 m/s (right panels). The total GRF recorded under both feet for each component (thick lines) is equal to the sum of the GRF recorded separately under each foot (plain thin lines) during the DC. The total GRF in each direction is equal to the force under the back foot at the front foot contact (0% of DC) and to that under the front foot at the back foot off (100% of DC). The decomposed GRF under each foot (dotted lines) is represented for each component. Note the similarity of the decomposed traces with those actually recorded under each foot for both normal and clinical gaits, even though the patient record shown here generated shear GRFs with different shapes and amplitudes than the healthy subject.

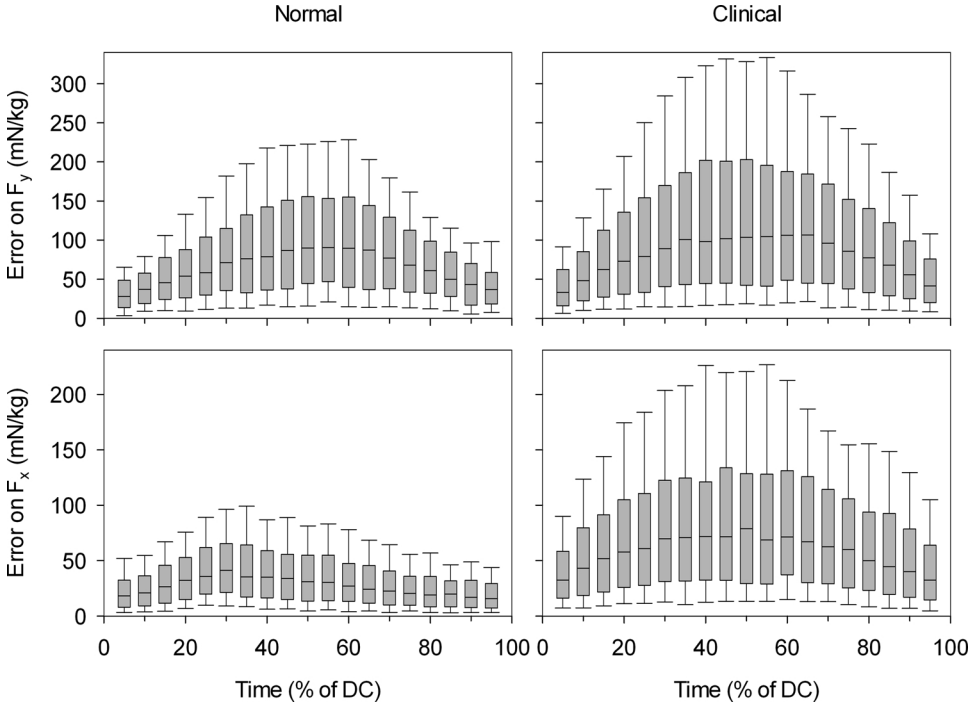

Fig. 4. Evolution of the normalized decomposition error on the fore-aft (F_y) and lateral (F_x) GRF components throughout the DC phase of walking in 374 steps of normal gait (left panels) and in 434 steps of clinical gait (right panels). Smaller errors are observed at the front foot contact (0% of DC) and at the back foot off (100% of DC), with a median error tripling on F_y around 50% of the DC and doubling on F_x around 30% of the DC in healthy gait and around 40% of the DC in clinical gait. Every 5% of DC, the median error is indicated as the box line, the 25th and 75th percentiles are indicated by the size of the box, the 5th and 95th percentiles are indicated by the whiskers.

Table 2
Error on the decomposition of shear GRF during the DC phase of walking.

GRF component	Normal					Clinical				
	p25	Median	p75	Mean	SD	p25	Median	p75	Mean	SD
Error on F_y (N)	3.21	4.59	6.47	5.25	2.91	2.10	3.27	5.7	4.23	3.01
Error on F_y (mN/kg)	46.6	64.4	92.4	75.0	42.2	52.4	84.8	126.7	101.9	67.5
Error on F_y (% of $F_{y,back}$)	2.2	3.0	4.1	3.3	1.6	4.7	7.7	13.4	10.8	9.7
Error on F_y (% of $F_{y,front}$)	1.9	2.7	3.6	2.9	1.4	4.1	6.6	10.7	8.8	7.2
Error on F_x (N)	1.44	1.93	2.64	2.22	1.17	1.54	2.43	3.81	3.18	2.57
Error on F_x (mN/kg)	20.6	28.4	39.1	31.7	15.7	40.6	61.7	96.0	75.7	51.3
Error on F_x (% of $F_{x,back}$)	3.9	5.7	10.2	7.7	5.4	7.2	12.0	19.2	15.6	13.6
Error on F_x (% of $F_{x,front}$)	2.1	3.0	4.5	3.4	1.7	4.7	6.8	11.7	8.6	5.7

GRF: ground reaction force; DC: double contact; p25: 25th percentile; p75: 75th percentile; SD : standard deviation.

This methodology differs substantially from existing alternatives [7,9–11] that approach the decomposition essentially as a curve fitting mission. Indeed, existing algorithms rely on the determination of the GRF under one foot as a mathematical function of time, parameterized to best fit the recorded force signals, ignoring any biomechanical interpretation and leaving aside the interrelations between forces and torques imposed by walking. The predictive model proposed to decompose the fore-aft GRF emphasizes the relationship between the fore-aft and vertical GRF imposed by the coordination of kinetic determinants of walking. The resulting complex force-time relation for $\hat{F}_{y,back}$ is modeled using 19 consecutive points predicted independently during the DC. Then, the decomposition of the lateral GRF relies strictly on a kinetic equation of the movement, avoiding mechanical inconsistencies between the decomposed and the recorded signals.

The fore-aft decomposition uses a machine learning process to build a predictive model that is robust, predicting new data with the same performance as learning data, and that is applicable to both normal and clinical GRFs. The counterpart to this robustness is a slight penalty in performance, resulting in a mean error of less than 3.3% in normal gait and of less than 10.8% in clinical gait. Compared to alternative methods [9–11] that hardly address robustness [9,10] and have not been applied to clinical gaits, the predictive decomposition of $F_{y,tot}$ demonstrates half of the error in the fore-aft GRF decomposition in healthy subjects. This outstanding performance suggests the existence of a predictable underlying relationship between $F_{y,back}$, $F_{y,tot}$ and $F_{z,back}$ that relies on the information captured in the GRFs during the DC phase of walking. For instance, speed and step length are captured in the GRFs, hence in the model, since higher speeds and shorter steps generate higher accelerations and decelerations at each step. Nonetheless, this relationship also holds in clinical gaits, including neurological and orthopedic pathologies, demonstrating body weight normalized errors of the same magnitude as in normal gait (less than 100 mN/kg on average). Larger relative errors in clinical gait can be explained by lower propulsion forces (average $F_{y,back}$ amplitude of 160 ± 40.5 N in normal gait and of 49 ± 30.1 N in clinical gait).

The lateral decomposition uses a biomechanical equilibrium, also applicable on left and on right steps and on normal and clinical gaits, implying that the decomposition performance strictly derives from the error in the estimated parameters used in the equation, namely $\hat{F}_{y,back}$, the center of pressure and the frictional torque under each foot. The lateral decomposition could be improved by a better knowledge of any of these variables. Indeed, a computation of the lateral decomposition when using the values actually measured for these variables in the equation provided a null error, which stems for the accuracy of this method. Another important feature of such biomechanical decomposition is that it is amenable to unfiltered signals. While most alternative methods use records filtered at 10 Hz [9] or even at 4 Hz [10], the biomechanical decomposition in lateral GRF captures the high force rates imposed by the transversal body weight shift that occurs during the DC especially at high speeds.

The decomposition of the shear GRF proposed in this study echoes the decomposition of the vertical GRF and the detection of the foot contact phases adapted to single platform measurement proposed by Meurisse et al [8]. Both methods outperform alternative decompositions by relying mostly on biomechanical equations of walking, while offering a performance unmatched to date. Together, these methods offer a 3D decomposition that can be used to analyze single foot parameters and detect asymmetries while both feet touch the same force platform or while walking on a single-belt instrumented treadmill. A quantitative gait assessment may also benefit from a reconstruction of the single-limb moments or center of pressure. The effect of the decomposition on joint torques computed in conjunction with kinematic measurements could be assessed in future research.

Declaration of competing interest

The authors have no conflict of interest to declare.

CRediT authorship contribution statement

Guillaume J. Bastien: Conceptualization, Methodology, Software, Validation, Formal analysis, Investigation, Resources, Data curation, Writing - review & editing, Visualization. **Thierry P. Gosseye:** Conceptualization, Methodology, Software, Validation, Formal analysis, Investigation, Data curation, Writing - review & editing, Visualization. **Massimo Penta:** Conceptualization, Methodology, Validation, Investigation, Writing - original draft, Writing - review & editing, Visualization, Supervision.

Acknowledgements

The authors are grateful to Christine Detrembleur for providing the clinical data and to Guillaume Meurisse for preparing a part of the data files.

References

[1] A. Rastegarpanah, T. Scone, M. Saadat, M. Rastegarpanah, S.J.G. Taylor, N. Sadeghein, Targeting effect on gait parameters in healthy individuals and post-stroke hemiparetic individuals, J. Rehabil. Assist. Technol. Eng. 5 (2018) 1–11.
[2] A.R. Altman, D.S. Reisman, J.S. Higginson, I.S. Davis, A kinematic comparison of split-belt and single-belt treadmill walking and the effects of accommodation, Gait Posture 35 (February 2) (2012) 287–291, https://doi.org/10.1016/j.gaitpost.2011.09.101.
[3] R. Kram, A.J. Powell, A treadmill-mounted force platform, J. Appl. Physiol. 67 (October 4) (1985) 1692–1698 1989.
[4] R. Kram, T.M. Griffin, J.M. Donelan, Y.H. Chang, Force treadmill for measuring vertical and horizontal ground reaction forces, J. Appl. Physiol. 85 (August 2) (1985) 764–769 1998.
[5] F. Dierick, M. Penta, D. Renaut, C. Detrembleur, A force measuring treadmill in clinical gait analysis, Gait Posture. 20 (December 3) (2004) 299–303.
[6] B.L. Davis, P.R. Cavanagh, Decomposition of superimposed ground reaction forces into left and right force profiles, J. Biomech. 26 (Apr-May 4-5) (1993) 593–597.

[7] L. Ballaz, M. Raison, C. Detrembleur, Decomposition of the vertical ground reaction forces during gait on a single force plate, J. Musculoskelet. Neuronal Interact. 13 (June 2) (2013) 236–243.
[8] G.M. Meurisse, F. Dierick, B. Schepens, G.J. Bastien, Determination of the vertical ground reaction forces acting upon individual limbs during healthy and clinical gait, Gait Posture. 43 (January) (2016) 245–250, https://doi.org/10.1016/j.gaitpost.2015.10.005 Epub 2015 Oct 17.
[9] D. Villeger, A. Costes, B. Watier, P. Moretto, An algorithm to decompose ground reaction forces and moments from a single force platform in walking gait, Med. Eng. Phys. 36 (November 11) (2014) 1530–1535, https://doi.org/10.1016/j.medengphy.2014.08.002 Epub 2014 Sep 16.
[10] B. Samadi, M. Raison, L. Ballaz, S. Achiche, Decomposition of three-dimensional ground-reaction forces under both feet during gait, J. Musculoskelet. Neuronal Interact. 17 (December 4) (2017) 283–291.
[11] E. Shahabpoor, A. Pavic, Estimation of tri-axial walking ground reaction forces of left and right foot from total forces in real-life environments, Sensors Basel (Basel) 18 (June 6) (2018) E1966, https://doi.org/10.3390/s18061966 pii.
[12] S. Weisberg, Applied Linear Regression, third edition, Wiley-Interscience, John Wiley & Sons, Inc., Hoboken, New Jersey, 2005.
[13] S. Arlot, A. Celisse, A survey of cross-validation procedures for model selection, Statistics Surveys, Institute of Mathematical Statistics (IMS) 4 (2010) 40–79.
[14] E. Halilaj, et al., Machine learning in human movement biomechanics: best practices, common pitfalls, and new opportunities, J. Biomech. 16 (November 81) (2018) 1–11.
[15] H. Xu, S. Mannor, Robustness and generalization, Mach. Learn. 86 (2012) 391, https://doi.org/10.1007/s10994-011-5268-1.
[16] J.J. Genin, P.A. Willems, G.A. Cavagna, R. Lair, N.C. Heglund, Biomechanics of locomotion in Asian elephants, J. Exp. Biol. 213 (March 5) (2010) 694–706, https://doi.org/10.1242/jeb.035436.
[17] J. Pozo, G. Bastien, F. Dierick, Execution time, kinetics, and kinematics of the maegeri kick: comparison of national and international standard karate athletes, J. Sports Sci. 29 (November 14) (2011) 1553–1561, https://doi.org/10.1080/02640414.2011.605164 Epub 2011 Oct 13.
[18] C. Detrembleur, A. van den Hecke, F. Dierick, Motion of the body centre of gravity as a summary indicator of the mechanics of human pathological gait, Gait Posture. 12 (2000) 243–250.
[19] A.E. Hoerl, R.W. Kennard, Ridge regression: biased estimation for nonorthogonal problems, Technometrics. 42 (February 1) (2000) 80–86.
[20] D.J. Schuirmann, A comparison of the two one-sided tests procedure and the power approach for assessing the equivalence of average bioavailability, J. Pharmacokinet. Biopharm. 15 (December 6) (1987) 657–680.
[21] J.L. Rogers, K.I. Howard, J.T. Vessey, Using significance tests to evaluate equivalence between two experimental groups, Psychol. Bull. 113 (May 3) (1993) 553–565.